



Silencing of LncRNA-ANCR Promotes the Osteogenesis of Osteoblast Cells in Postmenopausal Osteoporosis via Targeting EZH2 and RUNX2

Nuoya Cai^{1,2}, Chao Li³, and Fuke Wang⁴

¹Department of Respiratory, Qingdao Eighth People's Hospital, Qingdao, Shandong;

²Department of Orthopedic Surgery, Qingdao University, Qingdao, Shandong;

³Department of Tramatology and Orthopedics, Pingyi Hospital of Traditional Chinese Medicine, Linyi, Shandong;

⁴Department of Sports Medicine, the First Affiliated Hospital of Kunming Medical University, Kunming, Yunnan, China.

Purpose: This study aimed to explore the effects and mechanisms of long non-coding RNA (lncRNA) anti-differentiation non-coding RNA (ANCR) on the osteogenesis of osteoblast cells in postmenopausal osteoporosis (PMOP).

Materials and Methods: Mice models of PMOP were established. ANCR expression and intracellular calcium ions were detected by quantitative real-time polymerase chain reaction (qRT-PCR) and laser confocal microscopy, respectively. ANCR was silenced in osteoblast cells from PMOP mice by the transfection of siRNA-ANCR (si-ANCR). The proliferation and apoptosis of osteoblast cells was analyzed by MTT and flow cytometry, respectively. Alkaline phosphatase (ALP) activity and calcium nodules were examined by ALP and alizarin red staining assay, respectively. The expression of enhancer of zeste homolog 2 (EZH2), runt related transcription factor 2 (RUNX2), and OSTERIX was detected by qRT-PCR and Western blot. Furthermore, an osteogenesis model was constructed in mice, and osteoid formation was observed by hematoxylin-eosin (HE) staining. The interaction between lncRNA-ANCR and EZH2 was further identified by RNA pull-down assay.

Results: ANCR expression and intracellular calcium ions were increased in PMOP mice. Si-ANCR significantly increased the proliferation, ALP activity, calcium deposition of osteoblast cells and decreased apoptosis. ANCR and EZH2 were down-regulated by si-ANCR, while RUNX2 and OSTERIX were upregulated. Si-ANCR also promoted osteoid formation in mice treated with hydroxyapatite-tricalcium phosphate. In addition, ANCR specifically bound to EZH2.

Conclusion: Silencing ANCR promotes the osteogenesis of PMOP osteoblast cells. The specific binding of ANCR with EZH2 suppressed RUNX2, thereby inhibiting osteogenesis.

Key Words: Postmenopausal osteoporosis, osteoblast, lncRNA-ANCR, siRNA, EZH2, RUNX2

INTRODUCTION

Postmenopausal osteoporosis (PMOP) is a prevalent metabol-

Received: March 5, 2019 **Revised:** May 23, 2019

Accepted: June 16, 2019

Corresponding author: Fuke Wang, DM, Department of Sports Medicine, the First Affiliated Hospital of Kunming Medical University, No. 295, Xichang Road, Kunming, Yunnan 650032, China.

Tel: 86-0871-65376316, Fax: 86-0871-65376316, E-mail: wangfuke25@163.com

•The authors have no potential conflicts of interest to disclose.

© Copyright: Yonsei University College of Medicine 2019

This is an Open Access article distributed under the terms of the Creative Commons Attribution Non-Commercial License (<https://creativecommons.org/licenses/by-nc/4.0>) which permits unrestricted non-commercial use, distribution, and reproduction in any medium, provided the original work is properly cited.

ic bone disease characterized by bone loss and structural destruction, which increases the risk of fracture in postmenopausal women.¹ About 22 million women in the European Union and 8 million women in the United States have been diagnosed with osteoporosis.^{2,3} Owing to the high morbidity and serious complications of PMOP, many efforts have been devoted to its prophylaxis and treatment.^{4,5} However, women with osteoporosis still face high mortality due to the complications of fracture.⁶ Thus, deeper understanding of the pathogenesis of PMOP is vital for the clinical treatment thereof.

Osteoblast cells are specialized, terminally differentiated products of mesenchymal stem cells.⁷ By targeting inflammatory cytokines, osteoblast cells contribute to the process of bone formation.⁸ A previous study showed that osteoblast cells play

a very important role in the progression of PMOP via influencing bone anabolic function.⁹ Using primary cultured human osteoblast cells, Trošt, et al.¹⁰ indicated that the differential expression of certain genes is associated with the progression of osteoporosis. As one of the regulatory genes in organisms, the long non-coding RNAs (lncRNA)-anti-differentiation noncoding RNA (ANCR) is essential for osteoblast differentiation.¹¹ Jia, et al.¹² showed that the down-regulation of lncRNA-ANCR promotes osteogenic differentiation of periodontal ligament stem cells. Actually, the function of lncRNA-ANCR on osteoblast is complicated. Importantly, lncRNA-ANCR is associated with enhancer of zeste homolog 2 (EZH2), and the association results in the inhibition of both runt related transcription factor 2 (RUNX2) expression and subsequent osteoblast differentiation.¹³ This regulatory mechanism of lncRNA-ANCR has been observed in many diseases, such as breast cancer and colorectal tumor.^{10,14} However, whether lncRNA-ANCR can affect the occurrence of PMOP by regulating the osteogenesis of osteoblast cells is still unclear.

In the current study, osteoblast cells were isolated from a PMOP mice model and were transfected with siRNA-ANCR (si-ANCR). Subsequently, the proliferation, apoptosis, alkaline phosphatase (ALP) activity, and calcium nodules of osteoblast cells were analyzed. The expression of osteogenic differentiation related proteins was also investigated. Finally, the effect of si-ANCR on osteogenesis was evaluated in mice. In doing so, we aimed to explore the effects and mechanisms of lncRNA-ANCR on osteogenesis of osteoblast cells in PMOP to identify a new strategy for the treatment of PMOP.

MATERIALS AND METHODS

PMOP model construction

A total of 45 male KM mice (20–25 g, 7–8 weeks) were fed in a SPF grade environment at 25–27°C and 45–50% relative humidity. All mice cages were sterilized with 1:10000 perchloric acid. Meanwhile, bedding, water, and standard food were sterilized under high temperature and pressure. After 1 week of acclimatization, mice were randomly divided into three groups, including an osteoporosis group (n=15, undergo ovariectomy), a sham group (n=15, open/close abdomen operation without ovaries removed), and a control group (n=15, without any treatment). This study was approved by the local ethics committee, and all experiments were in accordance with the guide for the care and use of laboratory animals.

Primary cell culture

Soft tissue on the bone surfaces of PMOP mice was rapidly cleaned under aseptic conditions, and the intima was separated and cut into fragments. Then, these tissues were digested by trypsinase and incubated in a CO₂ incubator for 30 mins. After neutralizing trypsin, appropriate Roswell Park Memorial

Institute (RPMI)-1640 medium was added. The suction tube was repeatedly blown into cell suspension and inoculated in a culture flask. When osteoblast cells spread over 90% of the bottom of the bottle, they were digested and passaged with 2.5 g/L of trypsinase. Finally, the medium was removed, and the cells were washed with phosphate balanced solution (PBS) twice and detached from the plates with 0.25% trypsin. RPMI-1640 culture medium containing a 10% volume fraction of bovine serum was used to blow osteoblast cells into a single-cell suspension for routine passage.

Intracellular calcium ions measurement

Osteoblast cells were cultured in serum-free medium for 24 h to synchronize the cell cycle, followed by culturing in 10% fetal bovine serum (FBS) medium for 24 h. Osteoblast cells were washed twice with PBS buffer solution (supernatant removed) after adherence. Fluo8 was added to the plate with a solubility of 5 µm/mL, followed by removing the supernatant. Then, Tg solution was added to the plate at a final concentration of 4 µm/mL. After 40 min at room temperature away from light, the plate was washed twice with calcium-free PBS. Laser confocal microscopy was used to scan cells for 30 seconds. Finally, changes in calcium ions in osteoblast cells were scanned continuously after CaCl₂ solution (2 mM) injection.

Primary cell culture

Soft tissue on the bone surfaces of PMOP rats was rapidly cleaned under aseptic conditions, and the intima was separated and cut into fragments. Then, these tissues were digested by trypsinase and incubated in a CO₂ incubator for 30 mins. After neutralizing trypsin, appropriate RPMI-1640 medium was added. A suction tube was repeatedly blown into the cell suspension and inoculated in a culture flask. When osteoblasts spread over 90% of the bottom of the bottle, they were digested and passaged with 2.5 g/L of trypsinase. Finally, the medium was removed, and the cells were washed with PBS twice and detached from the plates with 0.25% trypsin. RPMI-1640 culture medium containing a 10% volume fraction of bovine serum was used to blow cells into a single-cell suspension for routine passage.

LncRNA-ANCR siRNA transfection

For transfection, osteoblast cells were divided into three groups, including si-ANCR (experimental group, cell line was transfected with si-ANCR), NC-ANCR (negative control group, cell line was transfected with lncRNA-ANCR negative control), and BLANK (blank control group, cells without treatment). Transfection was performed using Lipofectamine 2000 transfection kits (Invitrogen, Carlsbad, CA, USA), and all transfection operations were performed in strict accordance with Lipofectamine 2000 transfection instructions. Cells that were successfully transfected were prepared into cell suspension using Dulbecco's Modified Eagle Medium with 10% FBS and were

seeded at a density of 1×10^5 cells per well in 24-well plates, followed by incubation in a constant temperature incubator (5% CO₂, 37°C, 95% humidity). Then, the expression of lncRNA-ANCR was detected by quantitative real-time polymerase chain reaction (qRT-PCR) after transfection for 48 h.

The qRT-PCR detection

Total RNA was extracted and detected using RNAPrep Pure tissue kits (TIANGEN Biotech Co., Ltd, Beijing, China) and a NanoDrop ND-1000 Spectrophotometer (Thermo Fisher Scientific, Waltham, MA, USA), respectively. Meanwhile, cDNA was synthesized according to the instructions of the Takara PrimeScript RT reagent kit gDNA Eraser (TaKaRa Biotech, Kyoto, Japan) in accordance with the manufacturer's instructions. Then, qRT-PCR was performed on an ABI 7500 quantitative polymerase chain reaction system (Life Technologies Inc., Carlsbad, CA, USA). In detection of ANCR expression (forward, 5'-GCCACTATGTAGCGGGTTTC-3'; reverse, 5'-CCTGC GCTAAGAACTGAGG-3'), Runx2 expression (forward, 5'-CGGGTCTCCTTCCAGGAT-3'; reverse, 5'-GGGAACTGCTG TGGCTTC-3'), Osterix expression (forward, 5'-GAAGCGAC CACTTGAGCACAT-3'; reverse, 5'-TGTCCAAACTCATCAATG TATCT-3'), and EXH2 expression (forward, 5'-TTGTTGGCG GAAGCGTGAAAATC-3'; reverse, 5'-TCCCTAGTCCCGCG CAATGAGC-3'), the PCR program included 95°C for 10 min, 40 cycles of 95°C for 10 s, 60°C for 20 s, and 72°C for 34 s. GAPDH was used as an internal control (forward: 5'-CGAGCCA CATCGCTCAGACA-3'; reverse: 5'-GTGGTGAAGACGCCAG TGGA-3'). The experiment was repeated three times. The relative expression of target genes was calculated using the $2^{-\Delta\Delta Ct}$ method.¹⁵

Western blot

Osteoblast cells were lysed with 100 μ L/50 mL protein extract lysates. Briefly, after optical density (OD) was measured by a microplate reader (Varioskan LUX, Thermo Fisher Scientific) at 490 nm, proteins were separated by sodium dodecyl sulfate-polyacrylamide gel electrophoresis on 10% polyacrylamide gels and transferred to polyvinylidene fluoride membranes. After being blocked with 5% skim milk/BSA, the membranes were incubated with primary antibodies for EZH2 (1:1000, sc-131324, Santa Cruz Biotechnology, Delaware Ave Santa Cruz, CA, USA), RUNX2 (1:1000, sc-7177, Santa Cruz Biotechnology), OSTERIX (1:1000, cs-9272, Cell Signaling Technology, Inc., Boston, MA, USA), and glyceraldehyde-3-phosphate dehydrogenase (GADPH, 1:1000, sc-131325, Santa Cruz Biotechnology) overnight at 4°C. Then membranes were washed with Tris Buffered Saline Tween (TBST) and incubated with horseradish peroxidase-conjugated secondary antibody (1:5000, Shanghai Solar Biological Reagent Co., LTD., Shanghai, China). Protein bands were visualized using a gel imaging system (E-Gel Imager, Thermo Fisher Scientific).

MTT assay

The 3-(4,5-Dimethylthiazol-2-yl)-2,5-diphenyltetrazolium bromide (MTT) assay was performed to detect the proliferation of osteoblast cells. Simply, 200 μ L of osteoblast cells digested by trypsin were seeded in 96-well plates at a density of 6×10^3 /well. Then, 5 μ g of MTT (Cell Proliferation Kit I, Sigma Chemical Co., St. Louis, MO, USA) was added into each well. After 4 h of culturing, the medium was removed, and 150 μ L of dimethyl sulfoxide were added into each well. OD at 490 nm at different time points (0 d, 1 d, 2 d, and 3 d) was detected using a microplate reader (Varioskan LUX, Thermo Fisher Scientific), followed by MTT curve construction.

Apoptosis detection by flow cytometry

Flow cytometry was performed to detect the apoptosis of osteoblast cells. Simply, osteoblast cells were digested with trypsin, and then incubated with 200 μ L of Annexin V-FITC (BD Biosciences, San Jose, CA, USA) for 25 min and 10 μ L of propidium iodide (PI) for 15 min under darkness. Cell cycle progression was subsequently monitored based on flow cytometry (CytoFLEX, Cell Lab Quanta, Beckman Coulter, Kraemer Boulevard Brea, CA, USA), and data were analyzed using Multi-Cycle AV software, Version 6.0 (Phoenix Flow Systems, San Diego, CA, USA).

ALP staining assay

ALP staining was used for the ALP activity assay of osteoblast cells. Osteoblast cells were digested by trypsin and seeded in 24-well plates. Propanol (200 μ L, 15 min), incubation solution (200 μ L, 6 h), cobalt nitrate (200 μ L, 15 min), and ammonium sulfide (200 μ L, 5 min) were added successively. OD at 490 nm was detected using a microplate reader (Varioskan LUX, Thermo Fisher Scientific).

Alizarin red staining assay

The formation of calcium nodules was detected by alizarin red staining. Osteoblast cells were digested and seeded in 24-well plates. Polyformaldehyde (5%, 500 μ L, 10 min) and alizarin (200 μ L, 37°C, 30 min) were added to the medium successively, followed by photomicrographs for calcium nodules.

RNA pull-down assay

Transcription of lncRNA-ANCR was performed using T7 RNA polymerase (Thermo Fisher Scientific). lncRNA-ANCR was further labeled with biotin using biotin RNA Labeling Mix (Sigma Chemical Co.). Then the transcription product was purified using RNeasy Mini Kit (Qiagen, GmbH, Hilden, Germany) with DNase I (Qiagen). Totally, 1 μ L of labeled RNA in RNA structure buffer (10 mmol/L Tris pH7, 0.1 mol/L KCl, 10 mmol/L MgCl₂) was used for RNA secondary structure formation. Meanwhile, 3 μ g of osteoblast cells were harvested and lysed with RNA binding protein immunoprecipitation (RIP) lysis buffer (4°C, 1 h). Then, after centrifugation (12000 \times g, 4°C,

10 min), the remaining supernatant was mixed with 400 ng of biotin-labeled lncRNA-ANCR and 500 μ L of RIP buffer, followed by incubation for 1 h at 37°C. Afterwards, 50 μ L of streptavidin agarose beads (Invitrogen) were added into the supernatant for 1-h incubation. The level of lncRNA-ANCR was examined by qRT-PCR analysis based on RIP buffer washed liquid. Finally, Western blot was performed to detect binding between lncRNA-ANCR and genes.

Osteogenesis model construction

A total of 18 male immunocompromised mice (20–25 g, 4–6 weeks) was randomly divided into a si-ANCR group, NC-ANCR group, and BLANK group. Transfected cell lines ($1 \times 10^6/100 \mu$ L) were injected subcutaneously into the posterior limb implanted with hydroxyapatite-tricalcium phosphate (HA-TCP) mixture. Mice were killed 5 weeks after inoculation. Then, samples were fixed in 10% (v/v) formalin solution, dehydrated in ethanol, and processed routinely by embedding in paraffin. Finally, sections were used for hematoxylin-eosin (HE) staining and microscopic observation.

Morphological observation

Bone tissue of mice was fixed with 4% paraformaldehyde (Tianjin Institute of Chemical Reagents, Tianjin, China) for 24 h and decalcified with 20% formic acid and 15% ethylenediamine tetraacetic acid for 14 days. Followed by being embedded in paraffin, sliced (6 μ m), and stained with HE, pathological changes in bone tissue morphology were observed under a microscope.

Statistical analyses

All experimental data were expressed as mean \pm standard deviation (SD). Statistical analyses were performed by SPSS version 17.0 (SPSS Inc., Chicago, IL, USA) and GraphPad Prism 5.0 (GraphPad Software Inc., San Diego, CA, USA). Comparison between two groups was determined by t test. One-way analy-

sis of variance test was used for comparison among different groups. *p* values less than 0.05 were considered to be significantly different.

RESULTS

LncRNA-ANCR expression analysis

The PMOP model was established by bilateral ovariectomy in female mice. Six weeks after operation, the mice in the PMOP group showed significant decreases in bone mineral density, compared with the control group and sham group (Fig. 1A). Moreover, Fluo 8 staining and confocal laser microscopy were used to detect intracellular calcium ion levels in PMOP mice. Compared with the control group and sham group, intracellular calcium levels in the PMOP group were significantly lower (Fig. 1B), suggesting that the PMOP mouse model was successfully constructed. Furthermore, qRT-PCR analysis showed that the expression levels of lncRNA-ANCR in the PMOP group were significantly higher than those in the control group and sham group (*p*<0.001) (Fig. 1C).

The result of lncRNA-ANCR siRNA transfection

Osteoblast cells from PMOP mice were cultured and transfected with si-ANCR. qRT-PCR analysis showed that the expression levels of lncRNA-ANCR in the si-ANCR group was significantly lower than those in the NC-ANCR and BLANK groups (*p*<0.001) (Fig. 2), which further indicated that lncRNA-ANCR was silenced by si-ANCR in osteoblast cells.

Si-ANCR transfection promoted the proliferation and osteogenesis of osteoblast cells

The effect of lncRNA-ANCR inhibition on the proliferation of osteoblast cells was evaluated using MTT assay. Compared with the NC-ANCR group and BLANK group, the proliferation

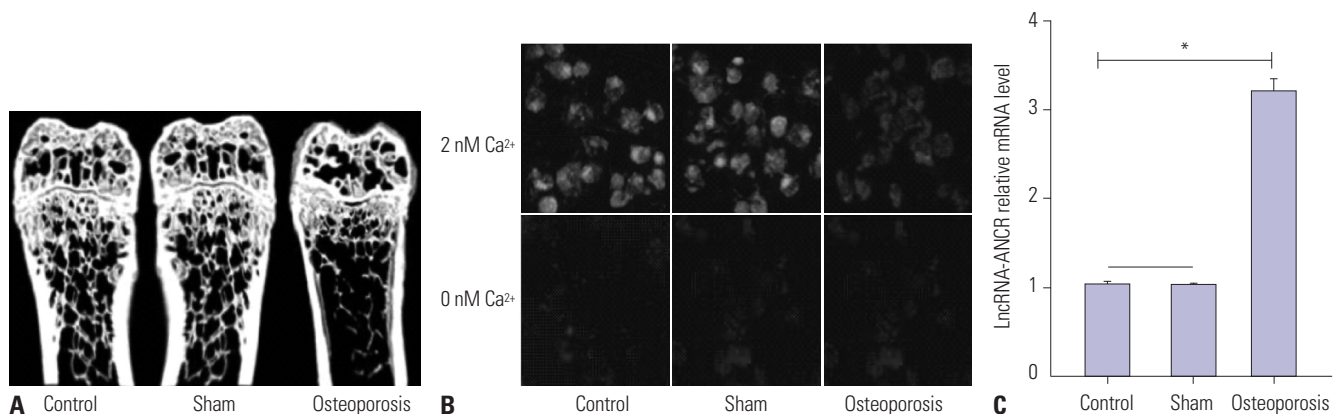


Fig. 1. Long non-coding RNA anti-differentiation noncoding RNA (lncRNA-ANCR) expression analysis based on a mouse postmenopausal osteoporosis (PMOP) model. The PMOP model was constructed using three groups: osteoporosis group, control group, and sham group (n=15 each group). (A) Bone mineral density comparison using microcomputed tomography. (B) Laser confocal microscopy detection for calcium level ($\times 100$, Fluo8 fluorescent probes are labeled). (C) Quantitative real-time polymerase chain reaction (qRT-PCR) analysis for lncRNA-ANCR mRNA and protein expression in osteoblast cells of the PMOP model. X-axis in C represents lncRNA-ANCR relative mRNA expression levels; Y-axis presents different groups in the PMOP model. **p*<0.001 vs. Control group and Sham group.

ability of osteoblast cells in the si-ANCR group was significantly increased ($p < 0.015$, Fig. 3A). Moreover, flow cytometry was used to detect the effect of lncRNA-ANCR inhibition on the apoptosis of osteoblast cells. The results showed that the apoptosis of osteoblast cells in the si-ANCR group ($2.3\% \pm 0.13$) were significantly lower than those in both the NC-ANCR group ($11.73\% \pm 0.15$) ($p < 0.001$) and BLANK group ($10.7\% \pm 0.12$) ($p < 0.001$) (Fig. 3B).

The effect of lncRNA-ANCR inhibition on ALP activity in osteoblast cells was detected using ALP staining. The result showed that the ALP activity (OD 490 nm) of osteoblast cells

was significantly higher in the si-ANCR group than in the NC-ANCR group and BLANK group at 14 and 21 days post-transfection ($p < 0.004$) (Fig. 3C). Furthermore, alizarin red staining showed that the transfection of si-ANCR significantly promoted the calcium deposition of osteoblast cells at 14 and 21 days post-transfection (Fig. 3D).

Si-ANCR transfection promoted osteoid formation in mice

Osteoblast cells were injected into the posterior limb of mice implanted with HA-TCP. HE staining showed that HA-TCP were greatly absorbed in the si-ANCR group, and a large number of red-stained osteoid-like tissues were observed. However, more HA-TCP remained in the NC-ANCR and BLANK group, and less osteoid-like tissues were observed (Fig. 4A). The osteoid/total area was significantly higher in the si-ANCR group than in the NC-ANCR and BLANK group ($p < 0.001$) (Fig. 4B).

Expression of EZH2, RUNX2, and OSTERIX after si-ANCR transfection

The expression of EZH2, RUNX2, and OSTERIX in osteoblast cells was detected by Western blot (Fig. 5). Compared with the NC-ANCR group and BLANK group, the expression of EZH2 in osteoblast cells of the si-ANCR group decreased significantly ($p < 0.001$), while the expression of RUNX2 and OSTERIX increased significantly ($p < 0.001$).

Interaction between lncRNA-ANCR and EZH2

RNA pull-down assay showed that ANCR could specifically bind to EZH2. However, ANCR-Mut, the truncated mutation

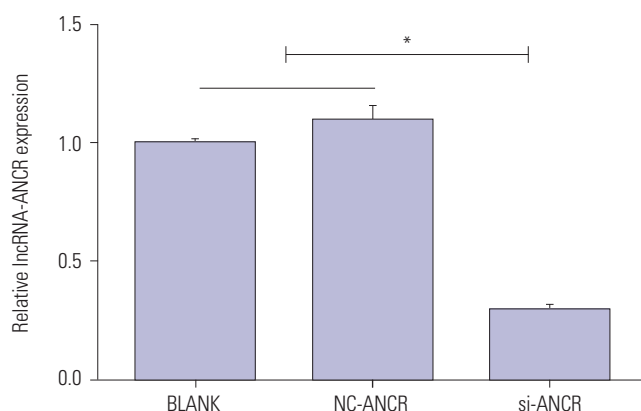


Fig. 2. mRNA expression of long non-coding RNA anti-differentiation noncoding RNA (lncRNA-ANCR) in osteoblast cells transfected with siRNA-ANCR (si-ANCR). X-axis presents relative lncRNA-ANCR expression; Y-axis presents the three groups in postmenopausal osteoporosis model. * $p < 0.001$ vs. NC-ANCR (negative control group, cell line was transfected with lncRNA-ANCR negative control) group and BLANK group (blank control group, cells without treatment).

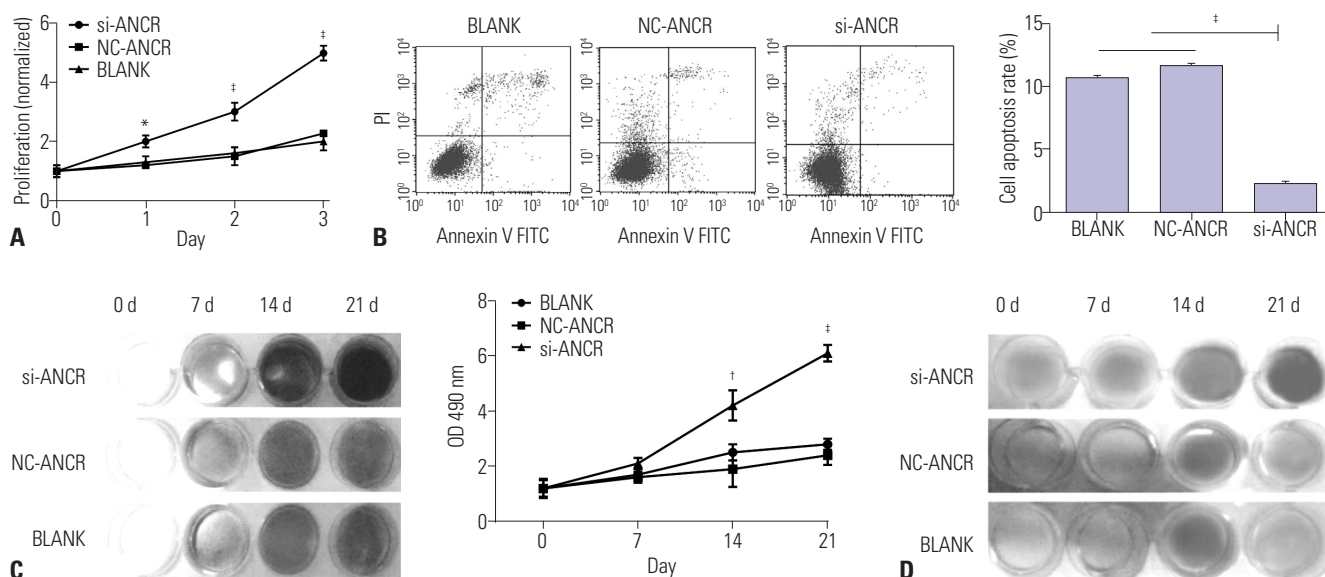


Fig. 3. Effects of long non-coding RNA anti-differentiation noncoding RNA (lncRNA-ANCR) transfected with siRNA-ANCR (si-ANCR). (A) The effect of lncRNA-ANCR on proliferation evaluated by MTT assay. (B) The effect of lncRNA-ANCR on apoptosis determined by flow cytometry. (C) The effect of lncRNA-ANCR on alkaline phosphatase (ALP) activity detected by ALP staining. X-axis represents the relative lncRNA-ANCR expression; Y-axis presents the three groups in the postmenopausal osteoporosis model. (D) The effect of lncRNA-ANCR on calcium deposition upon alizarin red staining. * $p < 0.05$, † $p < 0.01$, ‡ $p < 0.001$ vs. NC-ANCR group (negative control group, cell line was transfected with lncRNA-ANCR negative control) and BLANK group (blank control group, cells without treatment). PI, propidium iodide; FITC, fluoresceine isothiocyanate; OD, optical density.

control group, could not bind to EZH2 ($p < 0.001$) (Fig. 6A). Furthermore, antibodies binding to EZH2 exhibited significant ANCR enrichment, compared with non-specific antibodies ($p < 0.001$) (Fig. 6B).

DISCUSSION

In many individuals, bone mass homeostasis starts failing in

midlife, leading to bone loss, osteoporosis, and debilitating fractures.¹⁶ During this process, osteoblast cells play an important role in bone formation and differentiation.¹⁷ A previous study showed that osteoblast cells are closely associated with the development of diseases, such as prostate cancer, via regulating cell proliferation.¹⁸ In certain bone disease like multiple myeloma, the inhibition of osteoblast cells directly leads to the occurrence of bone lesions.¹⁹ A previous study indicated that osteoblast cells play a very important role in the progression

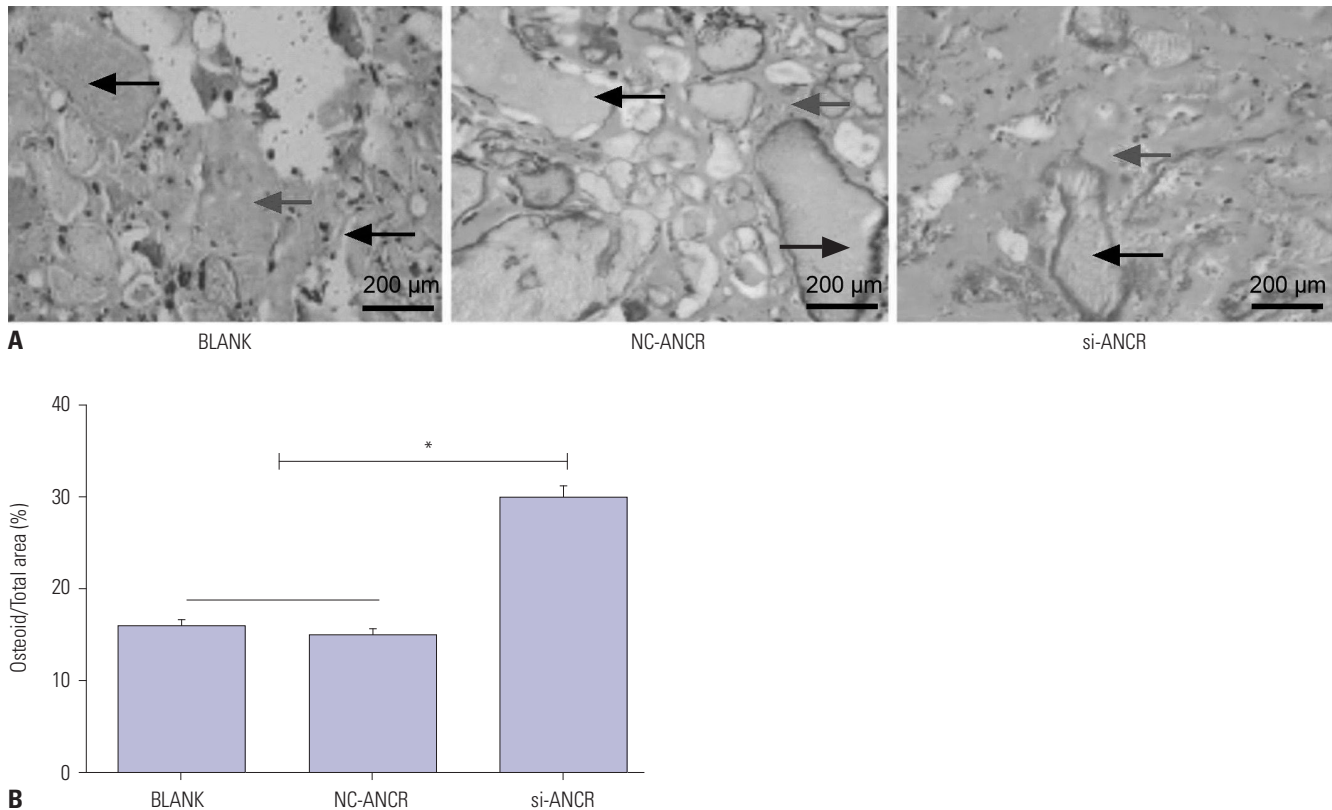


Fig. 4. In vivo experiments show the regulatory effect of long non-coding RNA anti-differentiation noncoding RNA (lncRNA-ANCR) on osteoid formation. (A) Hematoxylin-eosin (HE) staining of osteoid formation in mice injected with siRNA-ANCR (si-ANCR)-transfected osteoblast cells (bar=200 μm). Black and gray arrows indicate hydroxyapatite-tricalcium phosphate and osteoblast cells, respectively. (B) Osteoid/Total area (%). * $p < 0.01$ vs. NC-ANCR group (negative control group, cell line was transfected with lncRNA-ANCR negative control) and BLANK group (blank control group, cells without treatment).

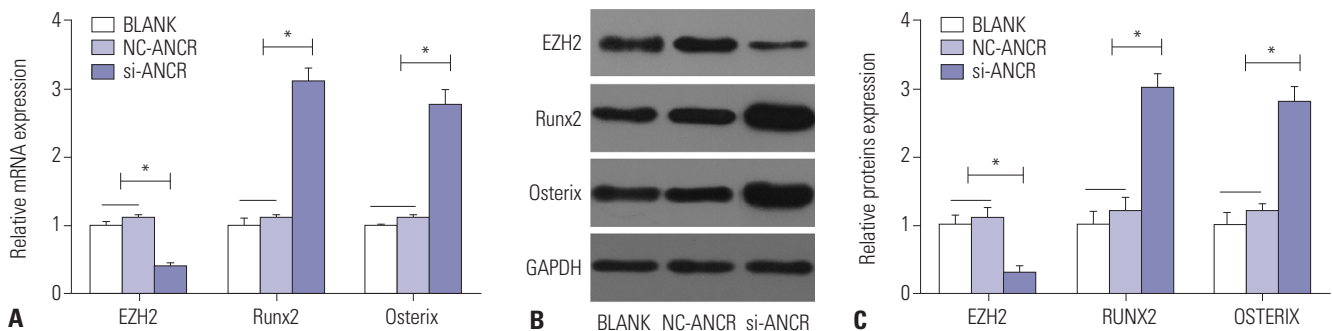


Fig. 5. Expression of enhancer of zeste homolog 2 (EZH2), runt related transcription factor 2 (RUNX2), and OSTERIX in osteoblast cells transfected with siRNA-anti-differentiation noncoding RNA (si-ANCR). (A) Quantitative real-time polymerase chain reaction (qRT-PCR) results for the mRNA and protein expression of EZH2, Runx2, and Osterix. (B and C) Western blot results for mRNA and protein expression of EZH2, RUNX2, and OSTERIX. * $p < 0.001$ vs. NC-ANCR group (negative control group, cell line was transfected with lncRNA-ANCR negative control) and BLANK group (blank control group, cells without treatment). GAPDH, glyceraldehyde-3-phosphate dehydrogenase.

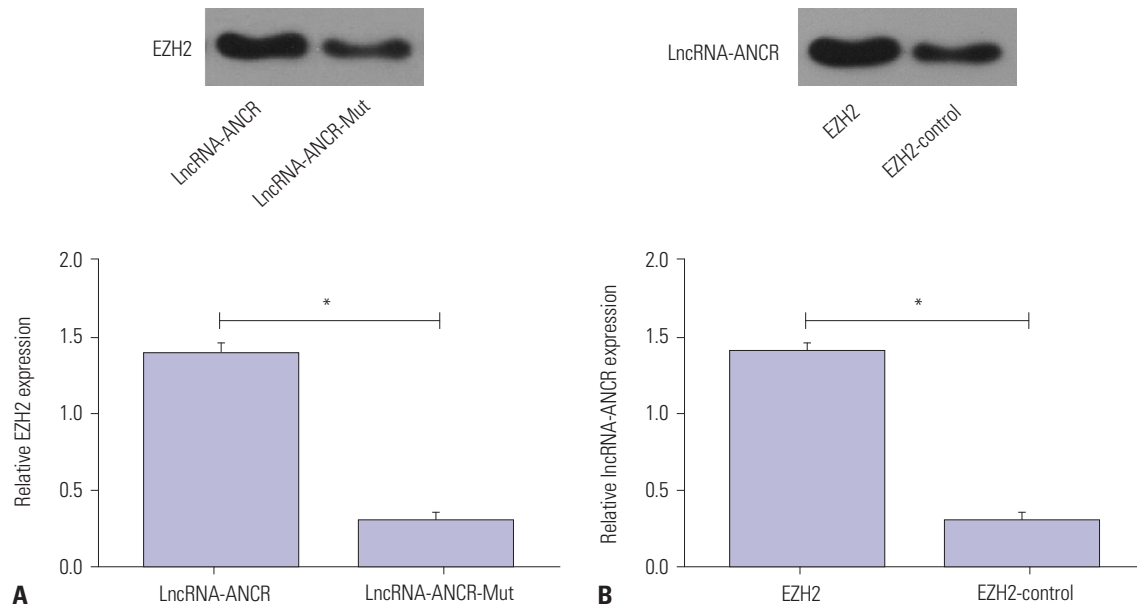


Fig. 6. The interaction between long non-coding RNA anti-differentiation noncoding RNA (lncRNA-ANCR) and enhancer of zeste homolog 2 (EZH2). (A) Expression of EZH2 in ANCR and ANCR-Mut detected by quantitative real-time polymerase chain reaction (qRT-PCR) and Western blot. (B) The expression of ANCR in EZH2 and EZH2-control detected by qRT-PCR and Western blot. * $p < 0.001$, lncRNA-ANCR group vs. lncRNA-ANCR-Mut group, EZH2 group vs. EZH2-control group.

of PMOP via influencing bone anabolic function.⁹ Actually, the dysregulation of lncRNA in osteoblast cells contributes to the progression of osteoporosis.²⁰ As one kind of lncRNA, lncRNA-ANCR is essential for osteoblast differentiation.¹¹ Jia, et al.¹² showed that the down-regulation of lncRNA-ANCR promotes osteogenic differentiation of periodontal ligament stem cells. However, the function of lncRNA-ANCR on the progression of PMOP is still unclear. In this study, qRT-PCR detection showed that lncRNA-ANCR is up-regulated in an osteoblast group based on the PMOP mice model, which further indicated that lncRNA-ANCR might take part in the development of PMOP. Moreover, siRNA can interfere with the expression of specific genes with complementary nucleotide sequences by degrading mRNA after transcription.²¹ To verify the function of target lncRNA in diseases, RNA interference has been established as an important biological strategy for gene silencing.²² A previous study showed that the silencing of tet methylcytosine dioxygenase 2 (TET2) by siRNA can be used to reveal the function of TET2 in bone marrow cells in myelodysplastic syndromes.²³ In the current study, compared with two control groups, osteoblast cells in the si-ANCR group showed a lower apoptosis rate, higher proliferation, and more stable calcium deposition. Thus, we speculated that silencing expression of lncRNA-ANCR might promote the osteogenic ability of osteoblast cells in PMOP.

EZH2 is a gene that participates in transcriptional repression.²⁴ It has been shown to be involved in establishing and maintaining gene repression through cell division.²⁵ A previous study showed that chromatin organization regulated by EZH2 is required for the migration of bone marrow-derived mesen-

chymal stem cells.²⁶ Chen, et al.²⁷ indicated that EZH2 regulates the differentiation of age-dependent mesenchymal stem cells into osteoblast cells. In mice models, EZH2 controls the bone formation and cell cycle progression during osteogenesis.²⁸ As a target gene, EZH2 is commonly regulated by lncRNA in cell proliferation in disease.²⁹ A previous study showed that the down-regulation of lncRNA-ANCR suppresses cell invasion and migration by regulating EZH2 expression.¹⁴ In breast cancer, the degradation of EZH2 mediated by lncRNA ANCR attenuated the invasion and metastasis of tumor cells.³⁰ In bone diseases, lncRNA-ANCR can regulate cell growth by interacting with the expression of EZH2.³¹ Moreover, RUNX2 is an important transcription factor necessary for osteoblast differentiation and bone formation.³² A previous study proved that RUNX2 induces osteoblast and chondrocyte differentiation and enhances their migration by coupling with PI3K-Akt signaling.³³ Actually, lncRNA can sponge miRNA to promote osteoblast differentiation through upregulating RUNX2.³⁴ Zhu, et al.¹³ indicated that downregulated lncRNA-ANCR promotes osteoblast differentiation by targeting EZH2 and regulating Runx2 expression. In this study, RNA pull-down analysis showed that lncRNA-ANCR could specifically bind to EZH2. Importantly, Western blotting in the current study showed that, compared with two other groups, the expression of EZH2 in osteoblast cells of the si-ANCR group decreased significantly, while the expression of RUNX2 and OSTERIX increased significantly. Based on these results, we speculated that the specific binding of lncRNA-ANCR with EZH2 inhibits the expression of RUNX2, thus inhibiting the osteogenesis of osteoblast cells in PMOP. However, there are some limitations in this study, such as the sample

size and lack of gene targeting drugs investigated based on lncRNA-ANCR. In addition, since osteoclast cells are also key in PMOP, the regulatory roles of lncRNA-ANCR on osteoclast cells were not analyzed. Thus, further research into these areas is needed.

In conclusion, lncRNA-ANCR may take part in the progression of PMOP. We found that silencing of lncRNA-ANCR promotes the proliferation and osteogenesis of PMOP osteoblast cells in vitro, as well as osteoid formation in vivo. Furthermore, the specific binding of lncRNA-ANCR with EZH2 inhibited the expression of RUNX2, thus inhibiting the osteogenesis of osteoblast cells in PMOP.

ACKNOWLEDGEMENTS

This work was supported by The Medical Science Leadership Training Program of Yunnan Province (D201639).

AUTHOR CONTRIBUTIONS

Conceptualization: Nuoya Cai. Data curation: Nuoya Cai. Formal analysis: Nuoya Cai. Funding acquisition: Chao Li. Investigation: Chao Li. Methodology: Chao Li. Project administration: Nuoya Cai. Resources: Nuoya Cai. Software: Chao Li. Supervision: Chao Li. Validation: Fuke Wang. Visualization: Fuke Wang. Writing—original draft: Nuoya Cai, Chao Li, and Fuke Wang. Writing—review & editing: Nuoya Cai, Chao Li, and Fuke Wang.

ORCID iDs

Nuoya Cai <https://orcid.org/0000-0001-8798-1494>
 Chao Li <https://orcid.org/0000-0002-1093-2595>
 Fuke Wang <https://orcid.org/0000-0002-9107-1765>

REFERENCES

- Black DM, Rosen CJ. Postmenopausal osteoporosis. *N Engl J Med* 2016;374:2096-7.
- Svedbom A, Hernlund E, Ivergård M, Compston J, Cooper C, Stenmark J, et al. Osteoporosis in the European Union: a compendium of country-specific reports. *Arch Osteoporos* 2013;8:137.
- Wade SW, Strader C, Fitzpatrick LA, Anthony MS, O'Malley CD. Estimating prevalence of osteoporosis: examples from industrialized countries. *Arch Osteoporos* 2014;9:182.
- Gennari L, Rotatori S, Bianciardi S, Nuti R, Merlotti D. Treatment needs and current options for postmenopausal osteoporosis. *Expert Opin Pharmacother* 2016;17:1141-52.
- Alami S, Hervouet L, Poiraudou S, Briot K, Roux C. Barriers to effective postmenopausal osteoporosis treatment: a qualitative study of patients' and practitioners' views. *Plos One* 2016;11:e0158365.
- Chang CY, Tang CH, Chen KC, Huang KC, Huang KC. The mortality and direct medical costs of osteoporotic fractures among postmenopausal women in Taiwan. *Osteoporos Int* 2016;27:665-76.
- Baum R, Gravalles EM. Bone as a target organ in rheumatic disease: impact on osteoclasts and osteoblasts. *Clin Rev Allergy Immunol* 2016;51:1-15.
- Shen F, Ruddy MJ, Plamondon P, Gaffen SL. Cytokines link osteoblasts and inflammation: microarray analysis of interleukin-17 and TNF- α -induced genes in bone cells. *J Leukoc Biol* 2005;77:388-99.
- Marie PJ, Kassem M. Osteoblasts in osteoporosis: past, emerging, and future anabolic targets. *Eur J Endocrinol* 2011;165:1-10.
- Trošt Z, Trebše R, Preželj J, Komadina R, Logar DB, Marc J. A microarray based identification of osteoporosis-related genes in primary culture of human osteoblasts. *Bone* 2010;46:72-80.
- Kretz M, Webster DE, Flockhart RJ, Lee CS, Zehnder A, Lopez-Pajares V, et al. Suppression of progenitor differentiation requires the long noncoding RNA ANCR. *Genes Dev* 2012;26:338-43.
- Jia Q, Jiang W, Ni L. Down-regulated non-coding RNA (lncRNA-ANCR) promotes osteogenic differentiation of periodontal ligament stem cells. *Arch Oral Biol* 2015;60:234-41.
- Zhu L, Xu PC. Downregulated lncRNA-ANCR promotes osteoblast differentiation by targeting EZH2 and regulating Runx2 expression. *Biochem Biophys Res Commun* 2013;432:612-7.
- Yang ZY, Yang F, Zhang YL, Liu B, Wang M, Hong X, et al. LncRNA-ANCR down-regulation suppresses invasion and migration of colorectal cancer cells by regulating EZH2 expression. *Cancer Biomark* 2017;18:95-104.
- Livak KJ, Schmittgen TD. Analysis of relative gene expression data using real-time quantitative PCR and the 2(-Delta Delta C(T)) method. *Methods* 2001;25:402-8.
- Harada S, Rodan GA. Control of osteoblast function and regulation of bone mass. *Nature* 2003;423:349-55.
- Ali AA, Weinstein RS, Stewart SA, Parfitt AM, Manolagas SC, Jilka RL. Rosiglitazone causes bone loss in mice by suppressing osteoblast differentiation and bone formation. *Endocrinology* 2005;146:1226-35.
- Logothetis CJ, Lin SH. Osteoblasts in prostate cancer metastasis to bone. *Nat Rev Cancer* 2005;5:21-8.
- Giuliani N, Rizzoli V, Roodman GD. Multiple myeloma bone disease: pathophysiology of osteoblast inhibition. *Blood* 2006;108:3992-6.
- Xiao X, Zhou T, Guo S, Guo C, Zhang Q, Dong N, et al. LncRNA MALAT1 sponges miR-204 to promote osteoblast differentiation of human aortic valve interstitial cells through up-regulating Smad4. *Int J Cardiol* 2017;243:404-12.
- McManus MT, Sharp PA. Gene silencing in mammals by small interfering RNAs. *Nat Rev Genet* 2002;3:737-47.
- Li G, Zou L, Xie W, Wen S, Xie Q, Gao Y, et al. The effects of NON-RATT021972 lncRNA siRNA on PC12 neuronal injury mediated by P2X7 receptor after exposure to oxygen-glucose deprivation. *Purinergic Signal* 2016;12:479-87.
- Shao Z, Zhang W, Fu R, Li L, Wang H. TET2 gene expression in bone marrow cells in myelodysplastic syndromes patients and the effect of silencing TET2 by siRNA on biological characteristics of healthy CD34+ cells. *Blood* 2012;120:4934.
- Tan JZ, Yan Y, Wang XX, Jiang Y, Xu HE. EZH2: biology, disease, and structure-based drug discovery. *Acta Pharmacol Sin* 2014;35:161-74.
- Ding X, Wang X, Sontag S, Qin J, Wanek P, Lin Q, et al. The polycomb protein Ezh2 impacts on induced pluripotent stem cell generation. *Stem Cells Dev* 2014;23:931-40.
- Liu L, Luo Q, Sun J, Ju Y, Morita Y, Song G. Chromatin organization regulated by EZH2-mediated H3K27me3 is required for OPN-induced migration of bone marrow-derived mesenchymal stem cells. *Int J Biochem Cell Biol* 2018;96:29-39.
- Chen YH, Chung CC, Liu YC, Yeh SP, Hsu JL, Hung MC, et al. Enhancer of zeste homolog 2 and histone deacetylase 9c regulate age-dependent mesenchymal stem cell differentiation into osteoblasts and adipocytes. *Stem Cells* 2016;34:2183-93.
- Dudakovic A, Camilleri ET, Paradise CR, Samsonraj RM, Gluscevic

- ic M, Paggi CA, et al. Enhancer of zeste homolog 2 (Ezh2) controls bone formation and cell cycle progression during osteogenesis in mice. *J Biol Chem* 2018;293:12894-907.
29. Wang D, Ding L, Wang L, Zhao Y, Sun Z, Karnes RJ, et al. LncRNA MALAT1 enhances oncogenic activities of EZH2 in castration-resistant prostate cancer. *Oncotarget* 2015;6:41045-55.
30. Li Z, Hou P, Fan D, Dong M, Ma M, Li H, et al. The degradation of EZH2 mediated by lncRNA ANCR attenuated the invasion and metastasis of breast cancer. *Cell Death Differ* 2017;24:59-71.
31. Zhang F, Peng H. LncRNA-ANCR regulates the cell growth of osteosarcoma by interacting with EZH2 and affecting the expression of p21 and p27. *J Orthop Surg Res* 2017;12:103.
32. Lucero CM, Vega OA, Osorio MM, Tapia JC, Antonelli M, Stein GS, et al. The cancer-related transcription factor Runx2 modulates cell proliferation in human osteosarcoma cell lines. *J Cell Physiol* 2013; 228:714-23.
33. Fujita T, Azuma Y, Fukuyama R, Hattori Y, Yoshida C, Koida M, et al. Runx2 induces osteoblast and chondrocyte differentiation and enhances their migration by coupling with PI3K-Akt signaling. *J Cell Biol* 2004;166:85-95.
34. Yu C, Li L, Xie F, Guo S, Liu F, Dong N, et al. LncRNA TUG1 sponges miR-204-5p to promote osteoblast differentiation through upregulating Runx2 in aortic valve calcification. *Cardiovasc Res* 2017;114: 168-79.